

## **X-RAY PHOTOELECTRON EMISSION, PHOTOLUMINESCENCE AND RAMAN ANALYSIS OF SOLID SOLUTIONS OF ALUMINIUM ZINC OXIDE**

**Mr.JAYARAM.P, Ms.JAYA.T.P, Mr.P.P. PRADYUMNAN\***

Department of Physics, University of Calicut, Calicut University(P.O.),  
Malappuram District,Kerala,India-673 635, Tele: 0494-2401144\*415,416,  
Fax: 0494-400 269

### **ABSTRACT**

High quality transparent conducting Al doped zinc oxide (AZO) powders were synthesised by solid state reaction route in different doping concentrations of Al (2%, 4%, 6%). Successful substitution of Al up to 6 wt% in ZnO lattice is confirmed from XRD pattern. The room temperature PL emission spectra shows two strong visible bands at 466nm (2.67eV) and 704nm (1.76eV). Raman scattering measurements exhibit the sample quality and specific aspects of lattice dynamics. A wide survey scan of XPS is taken in the range of 0-1100 eV.

**KEY WORDS:** Al doped zinc oxide, PL emission spectra, Raman spectra

### **1. INTRODUCTION**

Transparent Conducting Oxides (TCO) have been extensively used for various electronic and optoelectronic applications because of its very high transparency of visible light, absorbance of UV radiation and high IR reflectance. Besides these optical properties, the materials in the class of TCOs such as ZnO, In<sub>2</sub>O<sub>3</sub>, and SnO<sub>2</sub> shows high electrical conductivity [1, 2]. However it has been observed previously that undoped In<sub>2</sub>O<sub>3</sub> and ZnO possess considerable free charge carrier densities and the source of this conduction remains a mystery. ZnO shows a non stoichiometry with an oxygen deficiency up to 1% at equilibrium conditions [3-6]. In ZnO, previous studies have shown

that oxygen vacancies are donors, while Zn interstitials are too mobile to be stable at room temperature. Extrinsic doping of Group III elements produces n type conductivity in ZnO [5-7]. Among these, Al doped ZnO is widely studied in different potential applications including solar cells, flat panel displays, OLEDs, and optical coatings [8-10]. The behaviour of Al doped ZnO is dependent on the preparation conditions and the amount of doping. In the present study, structural, photoelectron emission and optical behaviour of AZO powder samples have been discussed. The samples are prepared by high temperature solid state reaction technique. The comparative studies of AZO powders at different concentrations are also reported. The complete XPS spectra and Raman analysis of the sample were done and the optical analysis is carried out by PL spectra. UV Vis spectrum supports the PL analysis.

## 2. EXPERIMENTAL

The experiment to synthesise high quality Al doped Zinc Oxide powder is carried out by high temperature solid state reaction technique with different doping concentrations of Al (2%, 4%, 6%). Appropriate quantities of Al<sub>2</sub>O<sub>3</sub> (99.999% purity) and ZnO (99.999% purity) were thoroughly ground for 3-4 hours to get a homogeneous mixture. The mixture is pelletized and sintered at 1000°C for 6 hours in a PID controlled high temperature furnace in oxygen atmosphere. The obtained pellets are again ground and the process is repeated several times in 2-3 steps in a temperature range of 1200- 1250°C for 24- 30 hours. Homogeneous powder samples of Al doped ZnO are obtained after this whole process. The crystallinity of the sample is ventured by X ray Diffraction using Cu-K  $\alpha$  of wavelength 1.54443 Å. The surface morphology is analysed using Scanning Electron Microscope equipped with a Schottky field emission source. X ray Photoelectron Emission spectrum is recorded by Thermo Scientific Multilab 2000 equipment to study the chemical composition of the samples. The optical studies were conducted using UV Vis transmission spectra taken using Perkin Elmer Lambda 35 Spectrometer and Photo Luminescence Spectra. The

molecular vibrations of the AZO powder were studied using Raman and IR Spectroscopy.

### **3. RESULTS AND DISCUSSIONS**

#### **3.1 Structural and Surface properties**

The XRD pattern of wurtzite ZnO is mostly preferred to orient in the (101) direction. The figure 1 shows the XRD of as synthesised Al doped ZnO at different wt% doping concentrations. From the present study it has been observed that all the prepared samples are of same phase and structure as that of hexagonal wurtzite structured ZnO [JCPDS 36-1451], and the reflections of the space lattice are indexed in the figure. For all concentrations of Al doping in ZnO, XRD shows the preferred (101) orientation and is in good agreement with previous reports [11-13]. The XRD pattern strongly shows the high crystalline nature of the Al doped ZnO. No peaks or secondary phase is observed either from Al<sub>2</sub>O<sub>3</sub> or from any other impurities, indicating that Al<sup>3+</sup> dopants occupied the position of Zn<sup>2+</sup> in the ZnO lattice as a substitutional atom. The effect of Al<sup>3+</sup> doping can be observed as a minute variation in the  $2\theta$  values of diffraction peaks and the lattice parameter values a and c. The crystallite size calculated by Sherrer formula [14], FWHM (deg), interplanar spacing (D) and lattice constants a (Å) and c (Å) were tabulated (table.1).

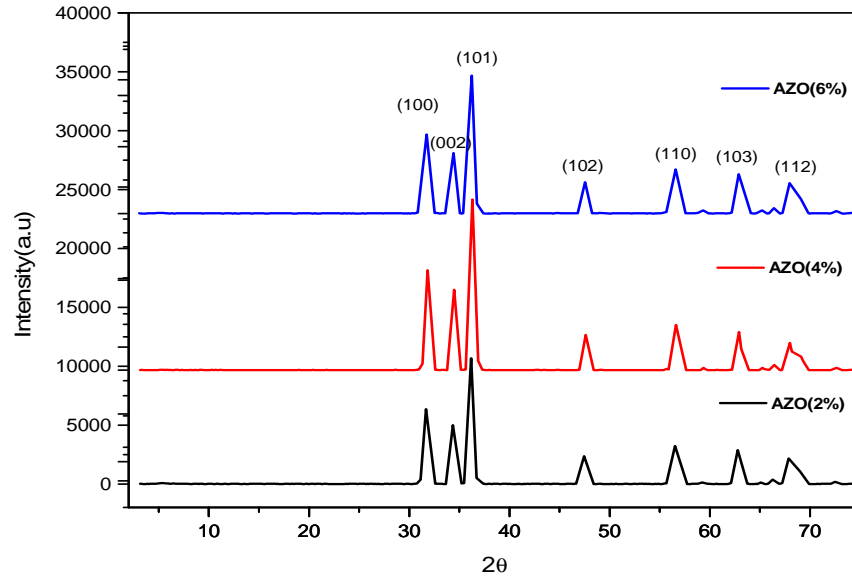


**Figure 1.** XRD patterns of Al doped ZnO and indices indicating the peak positions for the wurtzite hexagonal structure for different concentration of doping

**Table 1 :** Structural parameters calculated for different concentrations of Al in ZnO

Sample	$2\theta$ (deg)	FWHM (deg)	D( $\text{\AA}$ )	Crystallite size(nm)	Lattice constant a( $\text{\AA}$ )	Lattice constant c( $\text{\AA}$ )
2% Al	36.18	0.321	2.48073	27.07 nm	3.2556	5.2174
4% Al	36.319	0.282	2.47161	29.29 nm	3.2444	5.19623
6% Al	36.237	0.373	2.47695	22.41 nm	3.2513	5.2083

The surface morphology of the powders of Al doped ZnO was observed using SEM. Figure 2 shows the SEM images of the solid solution of Aluminum Zinc Oxide doped at (a) 2wt% (b) 4wt% (c) 6wt% of Al. It is observed that the particles are not of uniform size, varying in micro ranges and spherical in shape. There is no significant difference between the micrographs of the prepared samples.

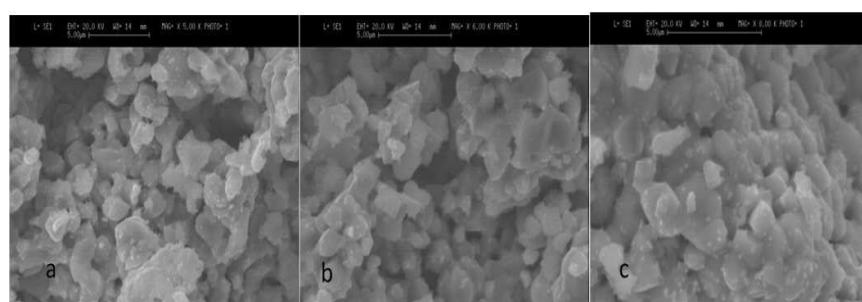


**Figure 2 : Surface Morphology of different powder (a) 2wt% Al (b) 4wt% Al (c) 6wt% Al in ZnO**

### **3.2 Optical Studies: UV-Vis and Photoluminescence Spectra**

The effect of Al doping in different concentrations on the optical properties of AZO was also investigated. Figure 3 shows the UV-Vis transmittance spectra. All the samples exhibit a transmittance of higher than 80% in visible region and absorption in UV-region. The visible transmission of these samples has been observed to increase slightly when Al concentration increases. The Al-doping enhances the optical transmittance of the ZnO and a significant variation can be observed from the plot when the concentration of Al doping increases from 2% to 4% and it further increases when it reach 6% of Al doping , which make them a suitable materials as the window layer for optoelectronic devices.

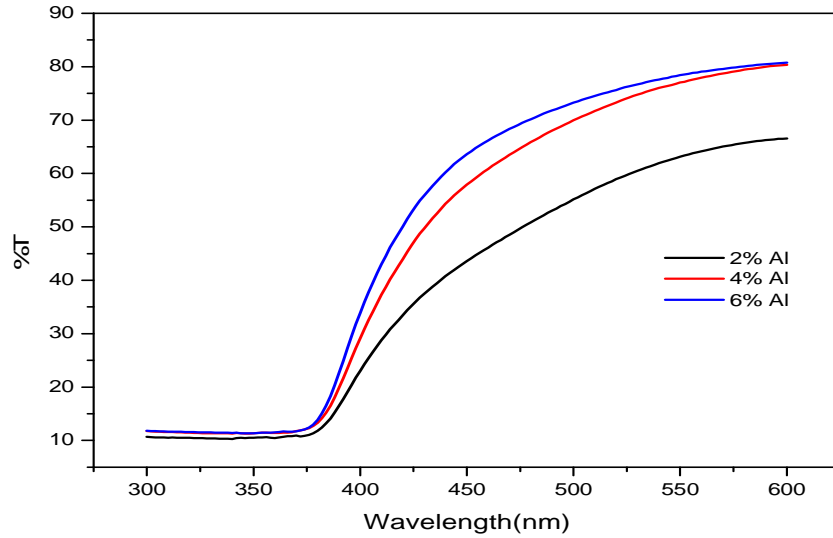


**Figure 3 : UV–Vis spectra shows variation of transmittance by Al doping concentration**

Figure 4 shows the room-temperature PL emission spectra of the AZO powders as a function of wavelength for three different  $\text{Al}_2\text{O}_3$  doping ratios with an excitation wavelength of 325 nm. Typical PL spectra of AZO consist of excitonic emission in the near-UV region and deep level emission in the green-blue region. Figure 4 exhibit two emission bands, two strong visible band about 466nm (2.67eV) and 704nm (1.76eV). The first strong emission (Figure 4.a) in the blue region can be attributed as the recombination of photoexcited holes with electrons occupying the singly ionized oxygen vacancies [15]. The formation of Al–O bonds in AZO may also produce this emission since Al ions exist in the form of  $\text{Al}^{3+}$  and Zn ions in the form of  $\text{Zn}^{2+}$ . When Al is incorporated in ZnO lattice, the Al ions will consume the residual O ions and decrease the concentration of interstitial oxygen in the AZO [16,17]. These two emissions can be regarded as the deep level emission due to oxygen defect in the material matrix and the high density crystalline nature of the samples. This study can be

regarded as a useful tool to investigate the defect in ZnO and Al doped ZnO ceramics.

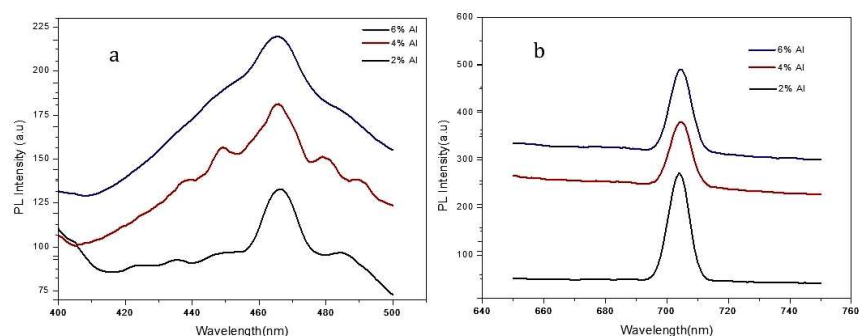


**Figure 4 : Room-temperature PLE spectra of the AZO powders**

Raman scattering measurements are well suited to obtain information about the sample quality in wide band gap semiconductors as well as to analyse more specific aspects of lattice dynamics. Figure.5 exhibit the Raman spectra and vibrational assignments of AZO powder sample prepared at all weight ratios. The A1 and E1 modes in Wurtzite structured ZnO are polar modes and are both Raman and Infrared active, whereas the E2 modes are non polar and Raman active only, having two frequencies associated with oxygen displacements and Zn sub –lattices. From figure it is evident that Al-doping in ZnO significantly lowered all the measured frequency regions as the doping concentration of Al was increased from 2wt% to 6wt% in the ZnO. The characteristic Raman frequency of wurtzite ZnO found at  $436\text{cm}^{-1}$  [18], showed a shift of  $(-8 \text{ to } +2 \text{ cm}^{-1})$  as the doping concentration increases. This can be regarded as the stress / strain induced by Al ions in the ZnO lattice.

The two intense sharp peaks at  $(327\text{-}329\text{cm}^{-1})$  and  $(428\text{-}438 \text{ cm}^{-1})$  can be attributed to the A1 (TO) and E2 mode vibrations. The prominent peak near  $333 \text{ cm}^{-1}$  corresponds to the second order scattering. The weak peaks at  $(517\text{-}537 \text{ cm}^{-1})$  are assigned to A1 (LO), and the other vibrations can be

assigned as shown in figure.5. ( $124-101\text{cm}^{-1}$ ) to E2, ( $202-207\text{cm}^{-1}$ ) to E2 and ( $660-674\text{cm}^{-1}$ ) to E1 (LO). The Raman Spectral intensity of the Al doped ZnO samples for 2%, 4% and 6% Al concentrations was significantly reduced in all of the measured frequency regions compared to that of the Undoped ZnO sample [19,20].The IR spectra of AZO was recorded in the transmittance mode. It is complimentary to the Raman spectra and exhibits characteristic bands between  $400$  and  $700\text{ cm}^{-1}$  as shown in Figure.6.

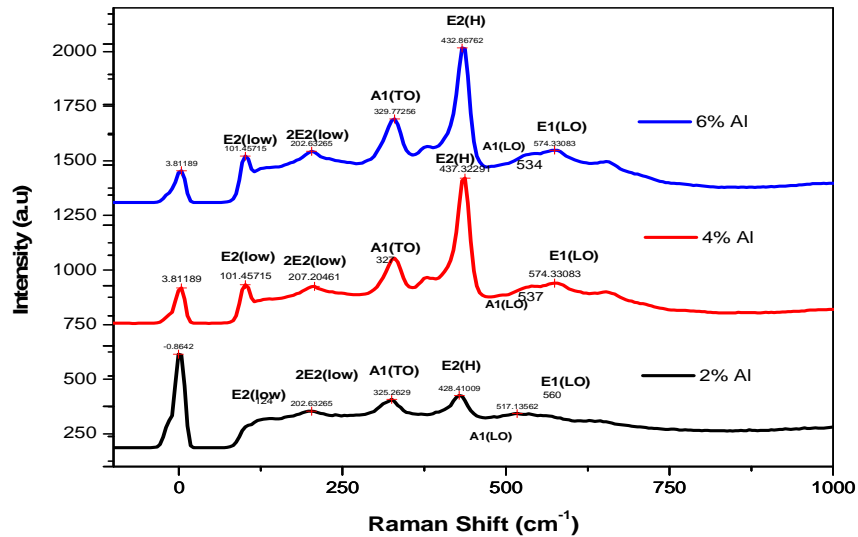


**Figure 5 : Raman spectra of AZO Samples in different wt% ratios**

A wide survey scan of XPS spectra is taken in the range of 0-1100 eV as shown in figure 6 From figure 6 the C 1s spectra shows a binding energy of 286.06 eV, usually used as an internal reference. The spectra corresponding to O 1s and Zn 2p core level of ZnO bulk sample is calibrated using binding energy of C1s. The lower binding energy component of Oxygen 1s at 532.99 eV is attributed to the Wurtzite structure of hexagonal  $\text{Zn}^{+2}$  ion of the metal oxide. The Zn 2p spectrum in the figure shows a doublet whose binding energies are 1022.54 and 1046.11 eV and can be identified as Zn 2p  $_{3/2}$  and Zn 2p  $_{1/2}$  lines

respectively. The binding energy difference between the two lines is 23.32 eV which is well according to the standard reference value of ZnO. The binding energy of the Al 2p is 74.74 eV as seen from the spectrum. The binding energy values confirm from the XPS spectra shows that the Zn atoms are in the +2 oxidation state [21-24].

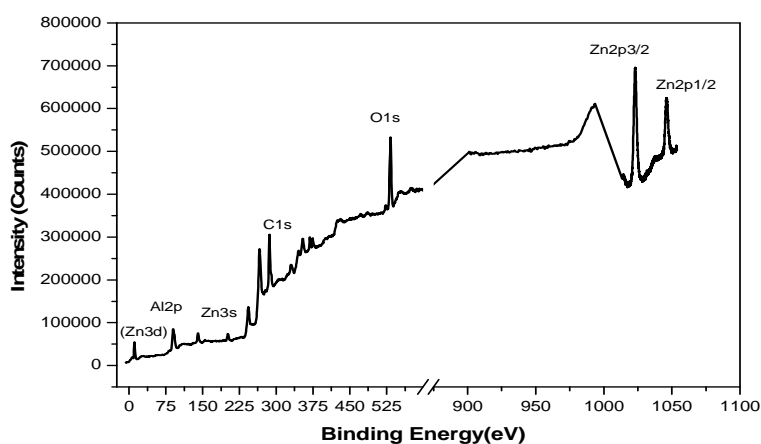


**Figure 6 : X-ray photoelectron emission survey spectrum**

#### 4. CONCLUSION

AZO bulk powders were successfully synthesized from the high purity powders of ZnO and Al<sub>2</sub>O<sub>3</sub> by solid state route. Successful substitution of Al at 6 wt% is reported with out affecting any structural damage to the wurtzite ZnO. The identity of the sample verified by XRD analysis confirms the perfect doping of Al in wurtzite ZnO lattice. No phase change or impurities were observed from the XRD spectra and it confirms the good quality of powder synthesized. Few reports have been made questioning the solubility of Al in ZnO, above 2% and the solubility of Al was found to decrease in some previous reports. Here we have synthesized a perfect solid solution of ZnO up to 6%. Wide range of characterization of the samples was reported after the confirmation of the

structural identity of the materials. There were no significant changes observed on the surface of material analyzed by SEM and the particles are micro sized. But significant changes were identified in the optical properties of the materials. The transmittance of the AZO bulk particles showed considerable variation of transmittance as the concentration of Al increases. The deep level emissions at blue and red regions provided information about the O defect in the material and it is worthy for future studies of stoichiometry of ZnO and AZO. The vibrational analysis done by Raman spectroscopy and the elemental composition was observed by X-ray Photoelectron emission spectra.

## 5. REFERENCES

1. J. H.W. de Wit (1975) , J. Solid State Chem. **13**, 192
2. J. Solid State Chem. **20**, 143 (1977)
3. J. H.W. de Wit, G. van Unen, and M. Lahey (1977) , J. Phys. Chem. Solids **38**, 819
4. L. E. Halliburton *et al* (2005) Appl. Phys. Lett. **87**, 172108
5. C. G. van de Walle (2000) Phys. Rev. Lett. **85**, 1012
6. D. C. Look *et al.* (2005) Phys. Rev. Lett. **95**, 225502
7. Stephan Lany and Alex Zunger (2007) PRL **98**, 045501
8. S. H. Jeong, B. N. Park, D. G. Yoo and J. H. Boo (2007), Journal of Korean Physical Society 50- 622-625.
9. J. Nishino, S. Ohshio and K. Kamata(1992) J. Am. Ceram. Soc. 75-3469-3472.
10. M. Chen, Z.L. Pei, C. Sun, J. Gong, R.F. Huang, L.S. Wen (2001) , Mater. Sci. Eng. B 85- 212.
11. Yang Zhang, Bixia Lin, Zhuxi Fu, Cihui Liu, Wei Han (2006) , Opt. Mater. 28-1192–1196.
12. M. Labeau, P. Rey, J.L. Deschanvres, J.C. Joubert, G. Delabouglise, (1992) Thin Solid Films 213-94.

13. S. Kumar, Y.J. Kim, B.H. Koo, H. Choi, C.G. Lee, (2009) JKPS 55 -1060–1064.
14. Xin Chen, Wenjie Guan, Guojia Fang, X.Z. Zhao, (2005) Appl. Surf. Sci. 252 ,1561–1567.
15. X.L. Wu, G.G. Siu, C.L. Fu, H.C. Ong, (2001) Appl. Phys. Lett. 78 , 2285.
16. L.E. Greene, M. Law, J. Goldberger, F. Kim, J.C. Johnson, Y. Zhang, R.J. Saykally, P. Yang, Angew. (2003) Chem. Int. Ed. 42 , 3031.
17. K. Vanheusden, W.L. Warren, C.H. Seager, D.R. Tallant, J.A. Voigt, B.E. Gnade, (1996) J. Appl. Phys. 79, 7983.
18. N. Ashkelon, et al (2003) ., J. Appl. Phys. 93 , 126.
19. H.W. Kim et al. (2010) Current Applied Physics 10 , 60–63
20. J. Das et al. (2010) Physica B 405 ,2492–2497
21. M. Chen et al. (2000) Applied Surface Science 158 ,134–140
22. K.C. Park, D.Y. Ma, K.H. Kim, 1997 Thin Solid Films 305 ,201.
23. R. Cebulla, R. Weridt, K. Ellmer, 1998 J. Appl. Phys. 83, 1087.
24. Z.Y. Ning, S.H. Cheng, S.B. Ge, Y., 1997, Thin Solid Films 307 ,50.